Nuclear-magnetic-resonance studies of hydrogen antitrapping effects by impurities (Mn,Cr,Fe) in zirconium dihydride

J-W. Han
Korea Standards Research Institute, Taedok Science Town, Taejon, Republic of Korea

D. R. Torgeson and R. G. Barnes
Ames Laboratory–U.S. Department of Energy and Department of Physics, Iowa State University, Ames, Iowa 50011

(Received 21 May 1990)

We report nuclear-magnetic-resonance measurements of the proton spin-lattice relaxation time T_1 in both pure and paramagnetic impurity-containing zirconium dihydrides. Measurements of the temperature dependence of the proton spin-lattice relaxation times T_1 were made on two series of ZrH_x samples (pure and impurity doped). The results show that paramagnetic impurities (Mn,Cr,Fe) contribute an additional spin-lattice relaxation rate R_{1p}, which is observed to increase in the sequence Fe→Cr→Mn and also to increase sharply with increasing hydrogen concentration at fixed impurity content in each case. The former result is consistent with the experimental results that the tendency towards localized moment formation in zirconium increases in the same sequence, whereas the latter may be accounted for by the antitrapping character of these impurities. Furthermore, the fit of R_{1p} data for the $ZrH_{1.97}$ sample doped with 500 ppm Mn or Cr yields an activation energy $E_a = 0.78$ eV/atom, which is ~75% of E_a in the bulk.

I. INTRODUCTION

It is well known that paramagnetic impurity ions play an important role in nuclear spin relaxation in insulating solids.[1] In earlier spin-relaxation measurements in metal hydrides, the paramagnetic impurity contribution, R_{1p}, to proton spin relaxation was usually neglected. However, recent investigations[2,3] have shown that as little as 10 parts-per-million (ppm) of such impurities can have profound effects on the spin-lattice relaxation rate.

Richards[4] has developed a general theory of relaxation of nuclear spins by paramagnetic ions, extending the earlier theories[1,5] to include the regime of atom diffusion as well as that of spin diffusion. The limiting cases of Richard's theory were used to account for the recent experimental results.[2,3] Because the proton-impurity interaction responsible for impurity-induced relaxation is of short range, R_{1p} is expected to be sensitive to the tendency of hydrogen to occupy sites in the vicinity of impurity ions. either favorably (trapping) or unfavorably (antitrapping).[3] Due to the short range of the proton-impurity interaction, the diffusion parameters in the vicinity of the impurity ions may be obtained through the rate, R_{1p}, whereas diffusion parameters in the bulk of the metal-hydrogen system can be determined by the diffusion-induced (dipolar) relaxation rate, R_{1d}.

The work reported here is an extension of the study of Mn and Fe impurities in titanium hydrides, TiH_x,[3] to zirconium hydrides, ZrH_x. In the study of Mn and Fe in TiH_x, it was shown that Mn supports a local moment in TiH_x and contributes an additional rate R_{1p} from which it was concluded that Mn is an antitrapping element with respect to hydrogen in TiH_x. On the other hand, Fe does not support a local moment in TiH_x. The occurrence or nonoccurrence of local moments by Mn and Fe is consistent with early magnetization studies of local moment formation,[6] which shows that, of the first-row elements, only Mn supports a local moment in Ti. That work also shows that Mn and Cr, but not Fe, retain local moments in Zr.[6] Accordingly, the present study of impurities in ZrH_x has included Cr as well as Mn and Fe as impurity elements.

II. THEORETICAL BACKGROUND

A. Proton spin-lattice relaxation rate

In metal hydrides, the measured spin-lattice relaxation rate may be written

$$R_1 = R_{1d} + R_{1e} + R_{1p} , \tag{1}$$

where the first term R_{1d} on the right side results from the proton-proton dipolar interaction, the second R_{1e} from the interaction between the protons and the conduction electrons, the last R_{1p} from relaxation by paramagnetic impurities. In the present investigation, the proton-^{91}Zr dipolar interaction is negligible due to the small magnetic moment and low abundance of ^{91}Zr.

B. Relaxation by dipolar and hyperfine interactions.

For the dipolar contribution, a simple exponential correlation function (or equivalently Lorentzian spectral density function) was suggested by Bloembergen, Purcell, and Pound (BPP).[7] According to this model, relaxation by proton-proton coupling can be written as

$$R_{1d} = \frac{3}{10}\gamma^4\hbar^2 \left[\frac{\tau_c}{1+\omega_0^2\tau_c^2} + \frac{4\tau_c}{1+4\omega_0^2\tau_c^2} \right] \sum_k r_k^{-6} , \tag{2}$$

where γ is the proton gyromagnetic ratio, $\hbar$ is Planck's constant, ω_0 is the proton Zeeman frequency, and τ_c is the correlation time. For proton-proton dipolar interaction, τ_c is given by $\tau_0/2$ where τ_0 is the mean dwell time of the proton at an interstitial site, r_k is the distance from the kth proton to a proton at the origin, and the sum is over all occupied interstial sites. As usual, τ_c is assumed to be thermally activated with $\tau_c=\tau_0\exp(E_a/k_BT)$, where E_a is the activation energy for hydrogen diffusion, k_B is the Boltzmann constant, τ_0 is a prefactor, and T is the absolute temperature.

Nuclear spin systems in metals, including metal hydrides are affected by the electronic structure of the metal through the hyperfine fields at the nuclei produced by conduction electrons. It has been shown[8] that the Korringa product[9] $T_{1e}T$ is generally weakly temperature dependent, particularly in systems that have a sharp structure in the density of states at the Fermi level. However, our measurements[10] of $T_{1e}T$ in zirconium hydrides at low temperatures (10–300 K) indicate that it is sufficient to approximate $T_{1e}T$ by a constant independent of temperature.

C. Relaxation due to paramagnetic ions

Nuclear spins diffuse via mutual spin exchange (spin diffusion) or atomic diffusion to the much larger electronic magnetic moments of the impurity where relaxation occurs via dipolar interaction or transferred hyperfine interaction. Because the dipolar interaction is dominant over the transferred hyperfine interaction in the systems under investigation, it will be assumed that the impurity-induced relaxation results primarily from the dipolar coupling between the proton and the paramagnetic ion. Because the dipolar field produced by the paramagnetic ion drops off as r^{-3}, those spins close to paramagnetic ions relax quickly via dipolar interaction. However, all the proton spins maintain a common spin temperature via their mutual nuclear spin-spin interaction. There are two important mechanisms for the transport of the excess energy in the nuclear spin system. Proton magnetization is transported to the paramagnetic ions (relaxation centers) by spin diffusion when hydrogen motion is frozen at low temperatures and by atomic diffusion at intermediate and high temperatures.

1. Spin-diffusion regime

In the spin-diffusion regime, according to Rorschach,[5] the spin-lattice relaxation process via the fluctuating dipolar fields of the impurity ions can be formulated as follows. A parameter C is introduced which measures the strength of the dipolar interaction between a nucleus and a paramagnetic ion, and which is defined by

$$\eta^{-1}(r)=Cr^{-6}\ , \tag{3}$$

where $\eta^{-1}(r)$ is the spin-lattice relaxation rate of a given nucleus due to the direct dipolar interaction with a paramagnetic ion fixed at a distance r. For a powder sample, C is given by[1]

$$C=\tfrac{2}{5}\gamma_p^2\gamma_n^2\hbar^2J(J+1)\left[\frac{\tau_i^*}{1+\omega_0^2\tau_i^{*2}}+\frac{7\tau_i^*}{3(1+\omega_e^2\tau_i^{*2})}\right]\ , \tag{4}$$

where J, γ_p, and ω_e are the total angular momentum, gyromagnetic ratio, and Larmor frequency of the paramagnetic ion, respectively, and γ_n is the gyromagnetic ratio of the nuclear spin (proton in the present case). $\tau_i^{*-1}=\tau_i^{-1}+\tau_H^{-1}$ where τ_i is the spin-lattice relaxation time of the impurity ion and τ_H, the smaller of the proton spin diffusion time, roughly the dipolar rigid lattice spin-spin relaxation time T_2, and the atomic diffusion dwell time τ_D. Because $\omega_e\gg\omega_0$, an approximation $\omega_e-\omega_0\simeq\omega_e$ was made in Eq. (4). The spin diffusion coefficient D_s characterizes the spin diffusion process, and was estimated by Bloembergen[1] to be $D_s=a^2/(50T_2)$ for a simple cubic lattice where a is the nearest neighbor distance between the protons. The pseudopotential radius β which describes the relative importance of the relaxation rates due to direct polar interaction and spin diffusion is defined as

$$\beta=(C/D_s)^{1/4}\ . \tag{5}$$

An additional parameter is the barrier radius b within which spin diffusion cannot occur. Near each paramagnetic ion, the magnetic field produced by an ion varies rapidly from site to site so that spin diffusion no longer occurs, since the Larmor frequencies of adjacent nuclei are sufficiently different to prevent mutual spin flips. b is defined by

$$b=(3\langle\mu_p\rangle/\mu_n)^{1/4}a\ , \tag{6}$$

where μ_n is the proton magnetic moment, and $\langle\mu_p\rangle$ is the average magnetic moment of the impurity ion given by

$$\langle\mu_p\rangle=\gamma_p\hbar J\left[B^2(x)+\frac{\partial B}{\partial x}\frac{2}{\pi}\tan^{-1}\left[\frac{2\pi\tau_i}{T_2}\right]\right]^{1/2}\ , \tag{7}$$

where $B(x)$ is the Brillouin function in which $x=\gamma_p\hbar JH_0/k_BT$. When the ion concentration is sufficiently low, the proton spin-lattice relaxation rate is given by

$$R_{1p}=8\pi ND_s\beta\frac{\Gamma(\frac{3}{4})}{\Gamma(\frac{1}{4})}\frac{I_{3/4}(\delta)}{I_{-3/4}(\delta)}\ , \tag{8}$$

where $I_m(\delta)$ is the modified Bessel function, $\Gamma(n/m)$ is the Gamma function, and δ is defined by $\delta=\beta^2/2b^2$.

2. Atomic diffusion regime

As the temperature increases, atomic diffusion becomes faster and transports the nuclear spins to the paramagnetic ion more efficiently than spin diffusion. It was first suggested by Shen[11] that D_s be replaced by the atomic diffusion coefficient D_a when the condition $D_a\gg D_s$ is satisfied in the fast diffusion limit ($\delta\ll1$). Richards[4] showed that this generalization also could be applied to Rorschach's Eq. (8). In this case, Eq. (8) can be written as

$$R_{1p}=8\pi N D_a \beta' \frac{\Gamma(\frac{3}{4})I_{3/4}(\delta_a)}{\Gamma(\frac{1}{4})I_{-3/4}(\delta_a)} , \quad (9)$$

where $\delta_a=\beta'^2/2a_1^2$, $\beta'=(C/D_a)^{1/4}$, and a_1 is the closest distance of approach of a hydrogen atom to a paramagnetic ion.

Although the paramagnetic impurity-induced relaxation in metal hydrides has been investigated previously,[2,3] quantitative analyses for their experimental results using Eqs. (8) and (9) were rather restricted since those equations are valid only in the limiting cases ($D_a \gg D_s$ or $D \ll D_s$). Because experimental results also occur in the intermediate regime in which D_s is comparable to D_a, a more general model is needed. Richard's[4] general model is valid for the entire range of temperature. The equations (8) and (9) are the limiting cases of this general expression, which can be written as

$$R_{1p}=8\pi N\beta(D_a+D_s)\frac{\Gamma(\frac{3}{4})}{\Gamma(\frac{1}{4})}\frac{qI_{3/4}(\delta)-I_{1/4}(\delta)}{qI_{-3/4}(\delta)-I_{1/4}(\delta)} , \quad (10)$$

where

$$q=\frac{\beta^2}{\beta'^2}(1+D_s/D_a)\frac{k_1}{k_2} , \quad (11)$$

with

$$k_1=I_{-1/4}(\delta')-\frac{I_{e/4}(\delta_a)}{I_{-3/4}(\delta_a)}I_{1/4}(\delta') , \quad (12)$$

$$k_2=I_{3/4}(\delta')-\frac{I_{3/4}(\delta_a)}{I_{-3/4}(\delta_a)}I_{3/4}(\delta') , \quad (13)$$

in which $\delta=\beta^2/2b^2$, $\delta'=\beta'^2/2b^2$, $\delta_a=\beta'^2/2a_1^2$, $\beta=[C/(D_a+D_s)]^{1/4}$, and $\beta'=(C/D_a)^{1/4}$. In the limit $D_a \ll D_s$, or $D_a \gg D_s$, Eq. (10) reduces to (8) or (9), respectively.

III. EXPERIMENTAL PROCEDURE

A. NMR measurements

Spin-lattice relaxation time measurements at 40 MHz were made in the Ames Laboratory with a phase-coherent pulsed NMR spectrometer. Measurements at temperatures from 10 to 300 K were made in a continuous flow helium cryostat which incorporated a home-built metal Dewar probe with a "Helitran LTD-3-110" transfer tube, cold finger, and control unit.[12] The metal Dewar was used to avoid unwanted proton resonance signals from hydrogen in the original Helitran Pyrex Dewar. In the home-built probe, the NMR coil is located within the Dewar chamber and contains only the sample tube so that the filling is significantly improved in comparison to the commercial unit in which the coil encloses the Dewar. The tuning circuit for the rf coil is located outside the Dewar at room temperature. Temperature control was achieved using a helium gas-blowing system with an Au-0.07% Fe thermocouple and a current feedback temperature controller. The sample temperature was monitored by a second Au-0.07% Fe thermocouple in contact with the sample but removed during data acquisition to reduce electrical noise. For measurements at temperatures above 300 K, a Pt/Pt-10% Rh thermocouple was used with a heater and a voltmeter null detector to feedback current to the heater power supply.

Spin-lattice relaxation times T_1 were measured using the inversion recovery pulse sequence 180-τ-90-FID with automatic incrementing of τ and signal averaging in a Nicolet 1170 digital signal averager.

B. Sample preparation

All samples were prepared from high-purity Ames Laboratory zirconium metal. The preparation began with the analysis of the very pure metals by spark-source mass spectroscopy. When the results of these analyses showed that the amount of paramagnetic impurities dissolved in the sample was negligible, as expected, the metal was carefully doped with other impurities (Mn,Cr,Fe) to form a metallic alloy. The metal (pure or doped) was heated to 943 K for high composition samples ($1.9<x<2.0$) and 1053 K for lower compositions to make hydride samples. Next the hydriding reaction was carried out by exposing the metal to the hydrogen gas, and the system was maintained to reach equilibrium for 24 h. After cooling, the residual pressure was carefully measured to determine the final composition. The sample was then crushed in a mortar in a helium filled dry box, filtered through a 200 mesh sieve and sealed in a quartz tube under low inert gas pressure.

IV. EXPERIMENTAL RESULTS

A. $Zr_{1-y}Mn_yH_x$ ($y=500$ ppm)

The spin-lattice relaxation time of the proton has been measured as a function of temperature in two series of zirconium dihydride samples. The first of these was prepared from nominal high-purity zirconium and consists of four samples $x=1.58$, 1.75, 1.86, and 1.98. The second was prepared from the purest zirconium available, alloyed with 550 ppm manganese and consists of four samples $x=1.57$, 1.75, 1.85, and 1.97. In the following, the results of T_1 measurements on these two sets of samples are displayed and their physical significance discussed.

As mentioned previously, there are several contributions to the measured total spin-lattice relaxation rate. Because these contributions are additive, it is not always possible to separate one from the others. In order to isolate the paramagnetic impurity contribution to the measured relaxation rate, the rate for the pure sample was subtracted from that of the impurity-doped samples. In this process, it was assumed that the parameters characterizing the bulk diffusion of the hydrogen atoms and the electronic structure of the samples are not affected by the presence of small amounts of impurity. In addition, small differences in hydrogen concentration ($\Delta x=0.01$) were assumed to be insignificant. According to this scheme, the impurity-induced relaxation rate R_{1p} can be written as

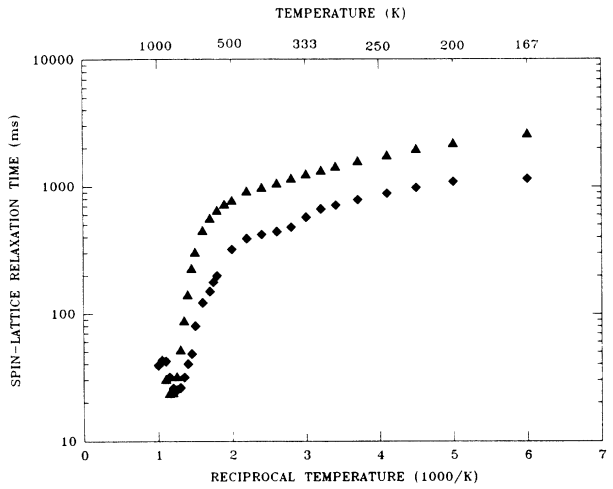

FIG. 1. Temperature dependence of the ^{1}H spin-lattice relaxation time at 40 MHz for pure $ZrH_{1.98}$ (solid triangles) and $ZrH_{1.97}$ doped with 500 ppm Mn (solid diamonds).

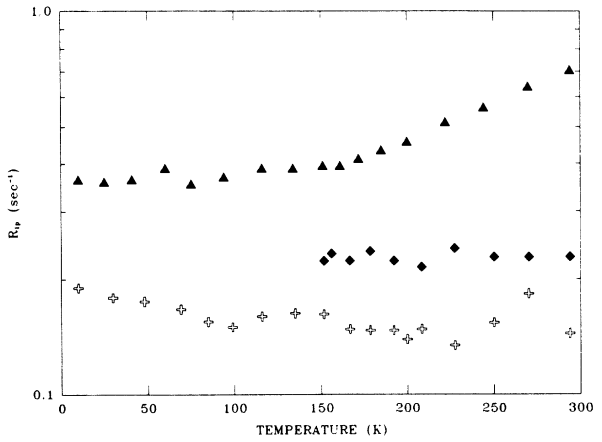

FIG. 3. Temperature dependence of the impurity-induced ^{1}H spin-lattice rate at 40 MHz for three different hydrogen concentrations in ZrH_x ($x = 1.97$, 1.85, 1.75) doped with 500 ppm Mn (solid triangles, diamonds, and open crosses, respectively).

$$R_{1p} = R_{1,\text{doped}} - R_{1,\text{pure}} , \tag{14}$$

where $R_{1,\text{doped}}$ is the measured relaxation rate for a sample containing a given amount of Mn and $R_{1,\text{pure}}$ the measured relaxation rate for a pure sample.

A composite plot of $\log T_1$ versus $1000/T$ at 40 MHz for pure $ZrH_{1.98}$ and for $ZrH_{1.97}$ doped with Mn is shown in Fig. 1. Also, Figs. 2 and 3 show composite plots of $\log R_{1p}$ versus $1000/T$ for the ZrH_x samples at 40 MHz. Because the paramagnetic impurity-induced rates are small compared to the rates due to the other contributions (especially the diffusion contribution at moderate and high temperatures), small experimental errors are amplified and reflected in the impurity-induced rates resulting in relatively large scatter in Fig. 2 except for the $ZrH_{1.97}$ sample.

Because the paramagnetic impurity-induced rate for the $ZrH_{1.97}$ sample is the largest and shows the least scatter, the experimental results for this sample are taken as an example for a quantitative analysis. The R_{1p} data plotted versus temperature are shown in Fig. 4. As a theoretical model for the fitting process, Richard's general expression[4] has been used. For quantitative analysis some of the characterizing parameters should be determined experimentally. First of all, the values of τ_i as a function of temperature are required. In principle, these values can be determined by electron spin resonance (ESR) measurements of the Mn^{2+} ion. This method has been successfully used[2] to determine τ_i of the Gd^{+3} ion, since this ion gives a strong ESR signal. However, the

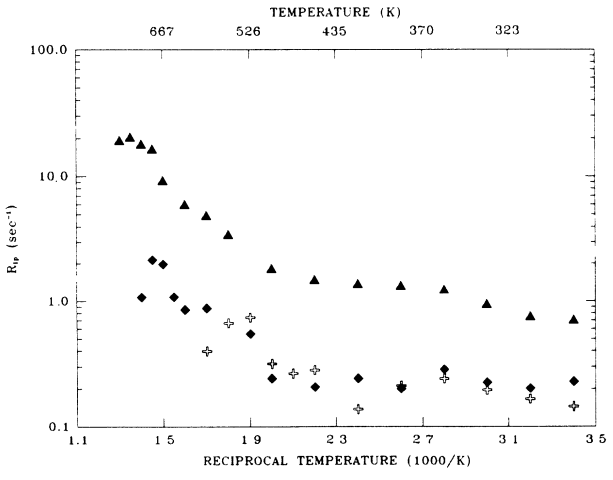

FIG. 2. Temperature dependence of the impurity-induced ^{1}H spin-lattice relaxation rate at 40 MHz for three different hydrogen concentrations in ZrH_x ($x = 1.97$, 1.85, 1.75) doped with 500 ppm Mn (solid triangles, diamonds, and open crosses, respectively).

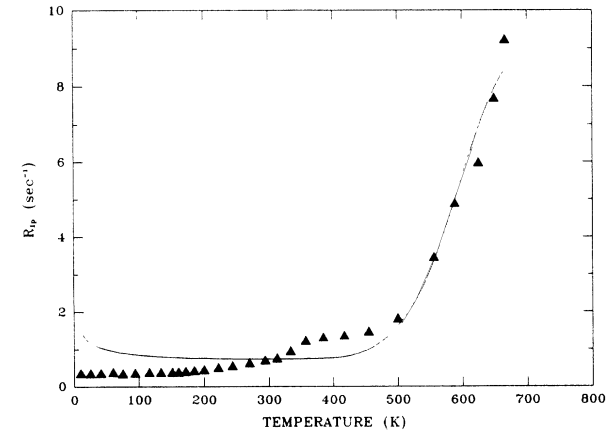

FIG. 4. Temperature dependence of the impurity-induced ^{1}H spin-lattice relaxation rate for $ZrH_{1.97}$ at 40 MHz. The solid line is a least-squares fit of Eq. (10) to the data.

weak signal of the Mn^{+2} ion, combined with noise from the quartz tube, which is believed to originate from some iron ions in it, made it difficult to use the same method. Thus, the experimental data have been fitted with adjustable parameters: the preexponential factor τ_0, activation energy E_a, for hydrogen motion near an impurity, and the Korringa constant[9] of the impurity ion, $\tau_i T = K_i$.

All other parameters have been determined and fixed as follows. The rigid lattice spin-spin relaxation time T_2 was determined to be 9.1 μsec from Bowman's measurements[13] of the second moment. The spin diffusion coefficient $D_s = a^2/(50T_2)$, for a simple cubic lattice where a is the nearest-neighbor distance between the protons.[1] Lowe and Gade[14] derived a more rigorous expression, $D_s = 0.15\gamma^2\hbar/a$, for a simple cubic lattice, which gives values about three times larger than Bloembergen's values.[1] Though these expressions are only valid for a simple cubic lattice, for our present purpose it is sufficient to use them for a slightly distorted simple cubic hydrogen sublattice in face-centered-tetragonal (fct) ZrH_x ($x \geq 1.7$). Using the latter expression, D_s was estimated to be 4.5×10^{12} cm^2/sec (a factor $x/2$ was taken into account to allow for incomplete occupancy of hydrogen sites). The nearest-neighbor distance between the protons a is 2.5 Å, and the impurity concentration was taken to have its nominal value of 500 ppm. Figure 4 shows the fit to the experimental data. The best fit parameters are the following: $\tau_i T = (4.8\pm1.6)\times10^{-9}$ sec K, $E_a' = (0.78 \pm 0.08)$ eV/atom, and $\tau_0 = (1.6\pm0.8)\times10^{-12}$ sec.

The value of $\tau_i T$ obtained from the fit is consistent with that deduced from ESR measurements[3] of Mn^{+2} ion in the gamma phase of titanium hydride ($\tau_i T = 2.5\times10^{-8}$sec K). This consistency is expected, since the properties of zirconium dihydrides are similar to those of titanium dihydride. From the fitted value of the parameter $\tau_i T$, it is evident that in the spin diffusion regime ($D_s \ll D_s$) the correlation time τ_i^* is determined entirely by the fluctuation rate of the impurity ion ($\tau_i \ll \tau_H$). From the temperature dependence of the values of the parameter δ (0.2 at 10 K, 0.18 at 540 K), it can be deduced that the system is in the fast spin-diffusion limit (weak interaction), in which the probability per unit time of the proton being relaxed by the impurity ion is much smaller than that of a spin diffusing away from the ion. This indicates that the bottleneck is the relaxation of the ion itself. As the temperature is increased, atomic diffusion becomes dominant over spin diffusion, and the barrier radius b becomes irrelevant. Accordingly, b should be replaced by the closest distance of approach ($a_1 = 2.1$ Å) of hydrogen to an ion. Replacement of b by a_1 ($b > a_1$) causes the spin system to pass from the fast spin-diffusion regime to the slow atomic diffusion regime ($\delta_s \gg 1$), in which the bottleneck is the atomic diffusion rate. Therefore, the relaxation rate $R_{1\rho}$ begins to increase sharply around 520 K reflecting a thermally activated diffusion process, as indicated by the increasing dependence of $R_{1\rho}$ on temperature in Fig. 4. The temperature of this changeover from weak to strong collision regime may be deduced from the condition $\tau_D \simeq T_2$. Based on the results of T_{1d} measurements for the pure $ZrH_{1.98}$ sample, the transition temperature is found to be 540 K, showing good agreement with the experimentally observed 520 K.

One striking result of the fit of $R_{1\rho}$ data is the low activation energy $E_a' = 0.78$ eV/atom, which is $\sim$75% of $E_a = 1.04$ eV/atom in the bulk where E_a has been determined from the analyses of the T_{1d} ($= R_{1d}^{-1}$) data. This result is qualitatively consistent with the observation in $Ti_{1-y}Mn_yH_x$.[3] When $D_a >> D_s$ Eq. (10) can be approximated by Eq. (9). Assuming that the temperature dependence of D_a is dominant over those of the Bessel functions and parameter C, E_s' may be deduced from the slope of the plot of $\log R_{1\rho}$ versus $1000/T$, and is expected to have an apparent activation energy $E_a' = 3E_a/4$. For the $Ti_{1-y}Mn_yH_x$ system, Belhoul *et al.*[3] obtained $E_a' = 0.11$ eV/atom in this way, which is $\sim$22% of E_a in the bulk. However, the activation energy deduced from the slope may be subject to relatively large errors resulting from the neglect of the temperature dependence of other terms, i.e., C and the Bessell functions in Eq. (9). This is supported by the fact that the activation energy inferred from the slope of the plot of $\log R_{1\rho}$ versus $1000/T$ for our system yields only 0.28 eV/atom, which is much smaller than the value of 0.78 eV/atom obtained from the fitting process.

These results appear to indicate that for this system the hydrogen diffusional motion is much faster in the vicinity of Mn ions that in the bulk. Belhoul *et al.*[3] suggested that the low activation energy may result from the short-range repulsive interactions between hydrogen atoms and Mn ions, which causes the potential wells to be shallower at hydrogen sites near Mn ions (antitrapping effect). Another possibility is that hydrogen atoms near Mn ions may form a highly localized solid solution phase, rather than the hydride phase in the bulk, and move faster in the former phase. Both pictures are supported by the observation that manganese does not form a hydride. This point will be discussed further in conjunction with the hydrogen-concentration dependence of $R_{1\rho}$.

As shown in Fig. 2, the maximum value of $R_{1\rho}$, and the temperature at which $R_{1\rho}$ has a maximum value, increase with increasing hydrogen concentration for the fixed 500 ppm Mn concentration. This behavior has been observed also in $Ti_{1-y}Mn_yH_x$.[3] $R_{1\rho}^{\max}$ occurs when the condition $\tau_D \eta^{-1}(a_1) \simeq 1$, or $\beta' \simeq a_1$, is fulfilled. This condition is equivalent to $C \simeq a_1^6/\tau_D$. At the temperature of the maximum for the $x = 1.97$ sample, the correlation time τ_1^* in C is entirely determined by τ_i, since τ_i is much smaller than τ_H as shown in Table I. In Table I, values for the $x = 1.75$ and 1.85 samples have been determined based on the assumption that the Korringa constants $\tau_i T$ for the $x = 1.75$ and 1.85 samples are not likely to be much different from that for $x = 1.97$. In this case, $T_{\max}$ depends on both τ_i and τ_D, and the condition $C = a_1^6/\tau_D$ may be written as $a_1^6/\tau_D = A[\tau_i + 7\tau_i/3(1+\omega_c^2\tau_i^2)]$ since $\omega_0\tau_i \ll 1$, where A is a constant. The values of a_1 have been determined from the hydrogen-concentration dependence[15] of the lattice parameters a and c with $a_1 = (2a^2 + c^2)^{1/2}$. Based on the weak dependence of the Korringa constant $\tau_i T$ and a_1 on hydrogen concentra-

TABLE I. Zirconium hydrides $Zr_{1-y}Mn_yH_x$ ($y = 500$ ppm).

x	T_{max}	τ_H at T_{max}	τ_i at T_{max}	a_1
1.75	526 K	6.4×10^{-8} sec	9.1×10^{-12} sec	2.07 Å
1.85	667 K	1.0×10^{-8} sec	7.2×10^{-12} sec	2.08 Å
1.97	740 K	2.2×10^{-8} sec	6.5×10^{-12} sec	2.07 Å

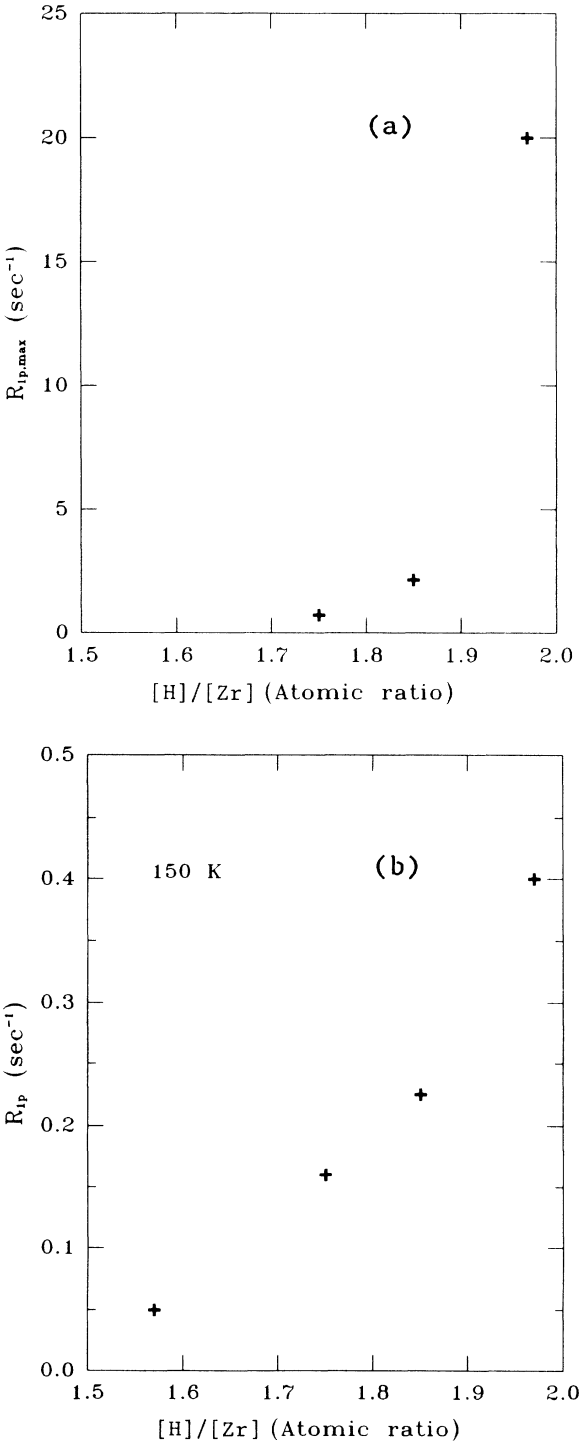

FIG. 5. (a) Hydrogen concentration dependence of R_{1p}^{max} in ZrH_x at 40 MHz. (b) Hydrogen concentration dependence of R_{1p} in ZrH_x at 150 K (40 MHz).

tion, the condition for R_{1p}^{max} is given by τ_D at T_{max} being constant, independent of hydrogen concentration. Therefore T_{max} is expected to increase with increasing hydrogen concentration, as experimentally observed, since the hydrogen hopping frequency decreases with increasing hydrogen concentration at a fixed temperature.

A more striking feature is the sharp increase of R_{1p}^{max} with increasing hydrogen concentration as shown in Fig. 5(a). Because the systems under investigation are in the atomic diffusion limit, Eq. (9) is the appropriate expression for R_{1p}. From the fact that at T_{max}, $\beta' = a_1$ and $\delta_a = \frac{1}{2}$, Eq. (9) can be rewritten as $R_{1p}^{max} N D_a a_1$ at T_{max}. With a fixed value of N and negligibly small hydrogen-concentration dependence of a_1, R_{1p}^{max} is proportional to D_a at T_{max}. Because D_a (or τ_D) at T_{max} is independent of hydrogen concentration as discussed before, R_{1p}^{max} is also expected to be independent of hydrogen concentration, contrary to the experimental observation. The experimental results may be accounted for by assuming that the hydrogen atoms avoid the vicinity of Mn ions (antitrapping effect) as suggested by Belhoul.[3] Thus, with increasing hydrogen concentration, it becomes more difficult for hydrogen atoms to avoid sites in the near neighborhood of Mn ions, and R_{1p}^{max} is expected to increase rapidly. Correspondingly, the previously mentioned highly localized solid solution phase is not likely to be the origin of the low activation energy near paramagnetic ions, since it would not cause the observed sharp increase of R_{1p}^{max} with increasing hydrogen concentration.

In the spin-diffusion limit, the sharp dependence of R_{1p} on hydrogen concentration is observed as shown in Fig. 5(b). Because R_{1p} stays nearly constant in this regime, τ_i is likely to satisfy both $\omega_e \tau_i \gg 1$ and $\omega_0 \tau_i \ll 1$. This is also confirmed by the value of $\tau_i T = (4.8 + 1.6)\times10^{-9}$ sec K with $\omega_e = 1.65\times10^{11}$ sec^{-1} and $\omega_0 = 2.5\times10^{8}$ sec^{-1} for Mn^{+2} in zirconium. With negligible variation of D_s as a function of hydrogen concentration, we may conclude that the hydrogen-concentration dependence of R_{1p} arises from either a change in τ_i or the antitrapping effect. $(\tau_i T)^{-1/2}$ is known to be proportional to the density of states at the Fermi level. NMR measurements[10,15–17] indicate that the d-band density of states has a local maximum at $x \simeq 1.8$. Thus, we may conclude that the observed behavior must be attributed to the antitrapping effect.

B. $Zr_{1-y}Cr_yH_x$ ($y = 500$ ppm)

The spin-lattice relaxation time of the proton has also been measured as a function of temperature in a series of zirconium dihydride samples ($x = 1.57$, 1.85, 1.97) prepared from the purest zirconium available, alloyed

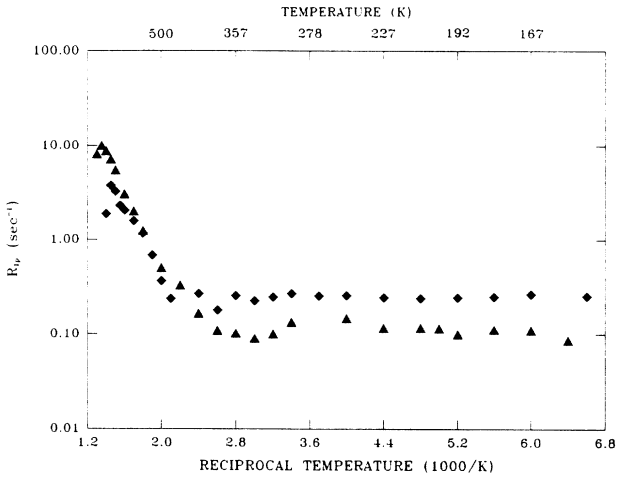

FIG. 6. Temperature dependence of the impurity-induced ^{1}H spin-lattice relaxation rate at 40 MHz for two different hydrogen concentrations in ZrH_x ($x=1.97$, and 1.85) doped with 500 ppm Cr (solid triangles and diamonds, respectively).

with 500 ppm chromium. Because the impurity-induced relaxation rate for $x=1.57$ is observed to be negligible, only the experimental results for the other two samples are presented and discussed here. Figure 6 shows a composite plot of $\log R_{1p}$ against temperature at 40 MHz for ZrH_x doped with 500 ppm Cr. A fitting procedure for one sample ($x=1.97$) has been carried out as previously described. The characterizing parameters are the following: $\tau_i T=(1.5\pm0.5)\times10^{-8}$ sec K, $E_a'=(0.79\pm0.08)$ eV/atom, and $\tau_0=(1.0\pm0.5)\times10^{-11}$ sec. The low activation energy E_a' of this system shows good agreement with that for the $x=1.97$ (500 ppm Mn) system, indicating that the Cr ion has similar effects on hydrogen. Furthermore, as shown in Fig. 6, $R_{1p}^{\max}$ rapidly increases with increasing hydrogen concentration as observed in the $Zr_{1-y}Mn_yH_x$ system. Accordingly, we may conclude that the low activation energy E_a' and sharp increase in $R_{1p}^{\max}$ result from the antitrapping character of Cr ion with respect to hydrogen. Comparing the relative magnitudes of $R_{1p}^{\max}$, we can infer information on the formation of localized magnetic moments of paramagnetic ions. The magnitude of $R_{1p}^{\max}$ in this system is smaller than that in $ZrH_{1.97}$ (500 ppm Mn) indicating that in the zirconium matrix, Mn forms a larger magnetic moment than do Cr ions.

In the spin-diffusion regime, it is seen from the calculated values of δ that this system is in the fast-diffusion limit. In contrast to the $Zr_{1-y}Mn_yH_x$ system, R_{1p} for the $x=1.85$ sample is observed to be greater than that for $x=1.97$ in the spin-diffusion regime (below 435 K). Similar behavior has been observed in the $Ti_{1-y}Mn_yH_x$ system.[3] At the present time, we do not have reasonable explanations for these experimental results.

C. $Zr_{1-y}Fe_yH_x$ ($y=500$ ppm)

We also measured the proton spin-lattice relaxation time T_1 in ZrH_x ($x=1.52$, 1.64, 1.93) samples doped with 500 ppm Fe to investigate the effects of the Fe ion on the proton T_1. In contrast to Mn and Cr ions, the effect of Fe is observed to be negligibly small. This result is consistent with the magnetic susceptibility measurements of Cape and Hake,[6] which showed that iron does not form a localized moment in zirconium.

V. SUMMARY AND CONCLUSIONS

Measurements of the temperature dependence of the proton spin-lattice relaxation time T_1 at 40 MHz have been made on two series of zirconium dihydride samples [pure and impurity-doped (Mn, Cr, Fe)]. The paramagnetic impurities contribute an additional spin-lattice relaxation rate R_{1p} which is observed to increase in the sequence Fe-Cr-Mn. This is consistent with the early finding[6] that the tendency towards formation of localized magnetic moments in zirconium increases in the same sequence. The activation energy E_a' near impurity ions obtained from the analysis of the impurity-induced relaxation rate is smaller than that in bulk zirconium. Furthermore, the maximum value of R_{1p} for the samples doped with Mn or Cr ions has been observed to increase sharply with increasing hydrogen concentration. These results may be accounted for by the antitrapping effect of impurity ions, which is believed to result from the interaction between these impurity ions and hydrogen atoms. This picture is consistent with the fact that both manganese and chromium do not form a hydride.

ACKNOWLEDGMENTS

The authors are indebted to B. J. Beaudry and A. Johnson for their careful preparation and analysis of the samples. Ames Laboratory was operated for the U. S. Department of Energy by Iowa State University under Contract No. W-7405-ENG-82. This work was supported by the Director for Energy Research, Office of Basic Energy Sciences.

[1]N. Bloembergen, Physica (Utrecht) **25**, 386 (1949).
[2]T-T. Phua, B. J. Beaudry, D. T. Peterson, D. R. Torgeson, R. G. Barnes, M. Belhoul, G. A. Styles, and E. F. W. Seymour, Phys. Rev. B **28**, 6227 (1983).
[3]M. Belhoul, G. A. Styles, E. F. W. Seymour, T-T. Phua, R. G. Barnes, D. R. Torgeson, R. J. Schoenberger, and D. T. Peterson, J. Phys. F **15**, 1045 (1985).
[4]P. M. Richards, Phys. Rev. B **18**, 6358 (1978).
[5]H. E. Rorschach, Jr., Physica (Utrecht) **30**, 38 (1964).
[6]J. A. Cape and R. R. Hake, Phys. Rev. **139**, A142 (1965).
[7]N. Bloembergen, E. M. Purcell, and R. V. Pound, Phys. Rev. **73**, 679 (1948).
[8]A. Narath, in *Hyperfine Interactions*, edited by A. J. Freeman and R. B. Frankel (Academic, New York, 1967).

[9]J. Korringa, Physica (Utrecht) **16**, 601 (1950).
[10]J.-W. Han, Ph.D. dissertation, Iowa State University, 1988 (unpublished).
[11]L. Shen, Phys. Rev. **172**, 259 (1968).
[12]L. R. Lichty, Ph.D. disseration, Iowa State University, 1988 (unpublished).
[13]R. C. Bowman, E. L. Venturini, and W.-K. Rhim, Phys. Rev. B **26**, 2652 (1982).
[14]I. J. Lowe and S. Gade, Phys. Rev. **256**, 817 (1967).
[15]C. Korn, Phys. Rev. B **28**, 95 (1983).
[16]R. C. Bowman, Jr., E. L. Venturini, B. J. Craft, A. Attalla, and D. B. Sullenger, Phys. Rev. B **27**, 1474 (1983).
[17]R. C. Bowman, B. D. Craft, J. S. Cantrell, and E. L. Venturini, Phys. Rev. B **31**, 5604 (1985).